NAVAL FACILITIES ENGINEERING SERVICE CENTER
Port Hueneme, California 93043-4370

Contract Report
CR-6129-OCN

ADDED MASS AND DAMPING CHARACTERISTICS FOR MULTIPLE MOORED SHIPS

by

David L. Kriebel, Ph.D., P.E.
Sarah Rollings, Ensign, USN
Bradley Hipp, Ensign USN

Ocean Engineering Program
United States Naval Academy
590 Holloway Road, Stop 11D
Annapolis, MD 21402

18 January 1999

Prepared for:
Commander, Surface Atlantic Fleet

19990429 077

Distribution is unlimited.

REPORT DOCUMENTATION PAGE

Form Approved
OMB No. 0704-0188

1. AGENCY USE ONLY (Leave blank)	2. REPORT DATE	3. REPORT TYPE AND DATES COVERED
	January 1999	Final

4. TITLE AND SUBTITLE

Added Mass and Damping Characteristics for Multiple Moored Ships

5. FUNDING NUMBERS

6. AUTHOR(S)

Kriebel, D., Rollings, S. and Hipp, B.

7. PERFORMING ORGANIZATION NAME(S) AND ADDRESS(ES)

United States Naval Academy
590 Holloway Road, Stop 11D
Annapolis MD 21402

8. PERFORMING ORGANIZATION REPORT NUMBER

CR-6129-OCN

9. SPONSORING/MONITORING AGENCY NAME(S) AND ADDRESS(ES)

Naval Facilities Engineering Service Center
1100 23rd Ave
Port Hueneme CA 93043-4370

10. SPONSORING/MONITORING AGENCY

11. SUPPLEMENTARY NOTES

12a. DISTRIBUTION/AVAILABILITY STATEMENT

Approved for public release; distribution is unlimited.

12b. DISTRIBUTION CODE

13. ABSTRACT (Maximum 200 words)

The Ocean Engineering Program, United States Naval Academy, conducted a series of tests for single ships and nests of 2, 3, 4 and 5 ships to determine the sway added mass and damping for ships moored in shallow water. This report documents the test program and test results.

14. SUBJECT TERMS

Ship Mooring, Added Mass, Damping

15. NUMBER OF PAGES

36

16. PRICE CODE

17. SECURITY CLASSIFICATION OF REPORT	18. SECURITY CLASSIFICATION OF THIS PAGE	19. SECURITY CLASSIFICATION OF ABSTRACT	20. LIMITATION OF ABSTRACT
U	U	U	U

EXECUTIVE SUMMARY

In heavy weather mooring (i.e. *Mooring Service Type III*) conditions ships in shallow water may be subjected to extremely dynamic conditions, such as caused by hurricane wind gusts or wind gust fronts. Very little is known about the added mass and damping characteristics of single or multiple moored ships in these types of conditions. Of special importance is the behavior of ships in the sway direction, because surface ships have relatively large broadside areas, so broadside wind forces may be particularly high.

Therefore, the Ocean Engineering Program, United States Naval Academy, conducted a series of tests for single ships and nests of 2, 3, 4 and 5 ships to determine the sway added mass and damping for ships moored in shallow water. This report documents the test program and test results.

These tests show that for nests of ships, the added mass and damping do not increase directly in proportion to the number of ships in the group, due to sheltering of one ship by another.

Water depth was found to be an especially critical parameter. The added mass can nearly double from deep water to a water draft-to-depth ratio of 0.95; the quadratic damping coefficient can increase nearly four fold from deep water to the shallowest depth tested with a draft-to-depth ratio of 0.95.

ADDED MASS AND DAMPING CHARACTERISTICS

FOR MULTIPLE MOORED SHIPS

By

David L. Kriebel, Ph.D., P.E.
Sarah Rollings, Ensign, USN
Bradley Hipp, Ensign USN

Ocean Engineering Program
United States Naval Academy
590 Holloway Road, Stop 11D
Annapolis, MD 21402

18 January 1999

Introduction

This report contains results of a set of laboratory experiments in which the dynamic sway motions of a "nest" of moored ships were simulated for shallow water conditions. A "nest" of ships is defined as a group of two or more ships moored together in a common mooring system. When a nest of ships is moored using a spread mooring, the entire group of ships will move as a rigid body in dynamic surge, sway, or yaw motions under the influence of wind, current, or wave forces. The dynamic motions of the group of ships will then depend on certain physical properties of the group, including the mass of the ships and the stiffness of the mooring system. These motions will also depend on the hydrodynamic properties of the system, such as the added mass of water entrained around the nest of ships and the viscous damping forces experienced by the group of ships.

This study was carried out at the request of the Naval Facilities Engineering Services Center to provide practical guidance on appropriate added mass and damping coefficients for use in simulating the behavior of multiple moored ships in shallow water. Traditional guidelines for the design of mooring systems are based primarily on a static analysis in which the added mass and damping characteristics of the moored ships are not taken into account. However, with the recent use of time domain computer simulation to predict the dynamic motions of moored ships, there is a need for empirical guidance on the magnitude of the added mass and damping. These methods require the user to input information about the viscous damping forces and added mass of a single ship, or for each ship in a nest of ships. At present, little information is available on how added mass or damping coefficients vary for a single ship in very shallow water; and, almost no data is available on these characteristics for multiple moored ships in any water depth.

To address these questions, a series of small-scale laboratory tests were conducted in the Naval Academy Hydrodynamics Laboratory (NAHL), with the goal of measuring the added mass and damping coefficients for nested ships in the lateral or sway mode of motion. These tests used existing models of a Yard Patrol craft, a 100-foot long vessel used at the Naval Academy to train Midshipmen in navigation and ship handling. Tests were performed using one ship, and using nests of two through five ships. Shallow water effects were evaluated through use of a fixed vessel draft together with four water depths. The tests were conducted by securing the nest of ships in a four-point mooring configuration, and then by giving the group of ships an initial displacement or offset from their at-rest position. Measurement of the subsequent damped dynamic motions permitted the added mass and damping characteristics of the system to be determined. The resulting data are presented graphically in order to identify trends in the behavior of added mass and damping coefficients as a function of the number of ships in the group and as a function of the relative water depth.

Dynamic Motions of Moored Ships

A single moored ship, or a group of moored ships, may experience dynamic movements in three modes of motion in the horizontal plane: surge, sway, and yaw. While it is of interest to determine the added mass and damping properties for each mode of motion, only the sway mode is considered here due to the limited scope of this study. While the other modes are of interest, added mass and damping are expected to be largest in the sway mode since the entire ship or nest of ships is moving broadside through the water.

Dynamic System with Linear Damping

Dynamic sway motions were considered through so-called "extinction tests" in which a group of ships, held in place with simulated mooring lines, was displaced horizontally from the at-rest position and was then released and allowed to return to the at-rest position through a series of damped dynamic oscillations. Analysis of the resulting data is based primarily on the mathematical model for a linear single degree of freedom (SDOF) system which represents the damped sway motions in the form:

$$(M + M_a)\,\ddot{y} + B\,\dot{y} + K\,y = 0 \tag{1}$$

where
$\dot{M}$ = mass of all ships in the group
M_a = added mass of all ships in the group
B = linear damping coefficient of the group
K = stiffness of the mooring system
y = sway displacement
$\dot{y}$ = sway velocity
$\ddot{y}$ = sway acceleration

For a linear system with relatively light damping, the lateral position of the group of ships as a function of time is expected to be given by:

$$y = Y_o\,e^{-\zeta t}\cos(\omega_d t) \tag{2}$$

where
Y_o = initial sway displacement at time $t=0$
ω_d = damped natural frequency of the system
ζ = exponential damping rate (dimensions of time^{-1})

Substitution of equation (2) into the equation of motion, in equation (1), then gives the following relationships among the various parameters:

$$\omega_d = \omega_n \sqrt{1 - \beta^2} \qquad (3)$$

$$\zeta = \beta \, \omega_n \qquad (4)$$

where
ω_n = undamped natural frequency of the system
β = exponential damping ratio (dimensionless)

and where these two parameters are defined by

$$\omega_n = \sqrt{\frac{K}{M+M_a}} \qquad (5)$$

$$\beta = \frac{B}{2\sqrt{K(M+M_a)}} \qquad (6)$$

In the experimental procedure, after the group of ships was released starting from an initial sway displacement, the damped natural frequency ω_d (equal to $2\pi/T_d$ where T_d is the damped natural period) and the decay rate ζ were determined by direct measurement. With these two experimental values known, equations (3) and (4) were solved for the undamped natural frequency, ω_n, and the damping ratio, β. Equation (5) was then solved for the added mass. In this study, the added mass is determined as a percentage of the total ship mass as

$$\frac{M_a}{M} = \frac{K}{\omega_d^2 M}(1-\beta^2) - 1 \qquad (7)$$

3

Dynamic System with Nonlinear Damping

Experimental data show that the damping in these extinction tests is not always linear, i.e. the motions do not always decay exponentially as suggested by the linear system in equations (1) through (6). In many tests, the motions would decay dramatically over the first several oscillations, but then would persist for a long period of time with minimal further decay and with an amplitude greater than that predicted by the linear damping model. These observations suggest that the actual damping is nonlinear in nature and, because the physical source of the damping is primarily viscous drag and flow separation, that damping may be represented by a quadratic function of velocity in the form

$$(M + M_a)\ \ddot{y} + B_{NL}\ \dot{y}\,|\dot{y}| + K\,y = 0 \tag{8}$$

where B_{NL} = nonlinear damping coefficient

The quadratic drag term is more commonly expressed in terms of a dimensionless cross-flow (sway) drag coefficient, C_D. By analogy to the drag force occurring on the ship in a steady flow, the nonlinear damping coefficient and the dimensionless drag coefficient may be related as

$$B_{NL} = N\ C_D\ \frac{1}{2}\ \rho\,L\,T \tag{9}$$

where
N = number of ships in the group
C_D = drag coefficient for lateral (sway) motion, per ship
ρ = density of water
L = ship length
T = ship draft

In this study, the lateral (sway) drag coefficient C_D is experimentally determined from the extinction tests of a group of moored ships. Because of the non-linear drag term, simple analytical solutions for the motions described by equation (8) are not available. As a result, equation (8) must be solved numerically for the time-dependent sway motions. This is accomplished using a finite-difference time-stepping solution. For this solution, the system mass, stiffness, and initial offset position were known. The added mass of the system was also known from the linear analysis described previously. As a result, the nonlinear damping coefficient was the only unknown and this was varied by trial and error to obtain what appeared to be the best fit of the measured damped oscillations.

4

Experimental Setup

Laboratory experiments were performed in the Stability Tank of the Naval Academy Hydromechanics Laboratory (NAHL). This tank is 20 feet long and 12 feet wide, and may be operated with any water depth of interest up to a maximum of about 3 feet. Four different water depths were used in these experiments: 4.2 inches, 5.7 inches, 8.0 inches, and 40.0 inches. All tests were conducted in still water.

Tests were performed using a set of five small-scale models of the Naval Academy Yard Patrol (YP) craft. The full-scale YP has a normal waterline length of 101.5 feet, a beam (at the deck level) of 24 feet, a draft of 6 feet, and a displacement of 167 long tons. Lines drawings for the full-scale YP are shown in Appendix A. The models used in this project were part of a systematic model test series conducted in the early 1980's and were constructed using a scale ratio of 1-to-20.24. All models therefore had a waterline length of 5.0 feet. The models were ballasted to a somewhat larger draft and displacement than would be normal. According to the scale ratio, the model draft and displacement should have been 3.56 inches and 44 lbs. In actuality, the models were ballasted to a common draft of 4.0 inches with an average displacement of about 49.75 lbs. The displacement and beam of each of the five models varied slightly. The average beam at the water line was 1.07 feet, but individual beams varied by as much as ten percent from this average value. Three of the models also had "soft" chine hulls while two models had "hard"chine hulls. Average characteristics of the five YP models as tested are listed in Table 1.

Table 1. Average Characteristics of YP models

Displacement (pounds)	Length (feet)	Draft (feet)	Beam (feet)
49.75	5.0	0.33	1.07

All tests were conducted with the models attached to a simple support frame as depicted in Figure 1. This frame consisted of thin wooden strips that were bolted to the deck level of the models near bow and stern. The model mooring lines (24-inch long rubber bands) were then attached to the ends of these wooden strips and to the side walls of the Stability Tank, thus simulating a four-point spread mooring configuration. By using the wooden support frame, the length of the rubber-band mooring lines could be kept constant for all tests, thus ensuring that the mooring stiffness did not change as the number of ships was changed.
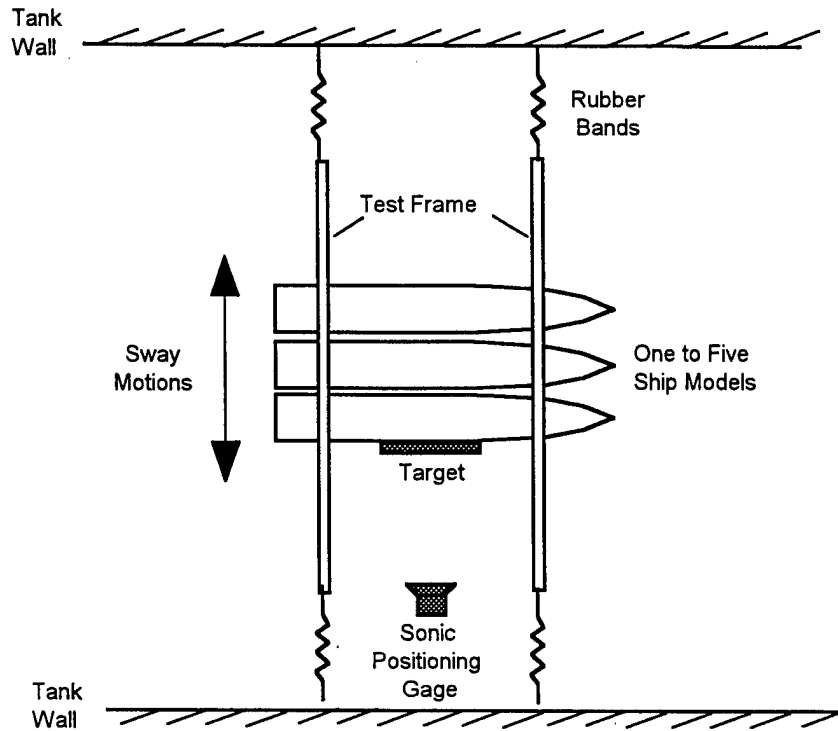
Figure 1. Illustration of Experimental Setup

Selection of Mooring Stiffness

The rubber bands used in the model mooring system were selected to produce a range of natural periods that would correspond to realistic values at full-scale based on Froude scaling laws. Guidance on the full-scale natural periods was provided, in part, by full-scale tests conducted on the *USS BARRY DD 933* (provided William Seelig, 1997, NFESC Draft Technical Note) in which the natural sway period for a destroyer moored to a pier was found to be about 60 seconds. Using the length scale ratio of 20.24, Froude model laws suggest a time scale ratio of $(20.24)^{\frac{1}{2}} = 4.5$. From the *BARRY* tests, a reasonable natural period at model scale would therefore be about 13 seconds. Various materials were investigated to simulate soft mooring systems. Rubber bands were finally selected as the simplest and most readily available materials that had sufficiently low stiffness to produce these long natural periods at model scale.

The stiffness, K, of these rubber bands was evaluated through two independent tests. The first test involved hanging weights from a 24 inch length of rubber band which was suspended vertically about eight feet above the floor. Weight was added in one-tenth of a pound increments, and the displacement or elongation of the rubber band was measured. This was carried out first using a single

6

rubber band, and was then repeated with two and three rubber bands in parallel. After completing the tests the weight was plotted verses the displacement, creating a set of load-deflection curves as shown in Figure 2 from which the stiffness may be evaluated as the initial slope.

As may be seen, the load-deflection curves defined by the data points was not perfectly linear, but rather was slightly curved with proportionally more incremental displacement with the incremental addition of weight. Based on some trial tests with the ship models connected to the rubber bands in the Stability Tank, it was found that model displacements of less than 6 inches would be used for subsequent model tests. As a result, the stiffness of the rubber bands was determined as the slope of load-deflection curves over the first 6 inches of displacement. The stiffness for a single rubber band was then found to be 0.52 lb/ft. As expected, this value doubled for two rubber bands in parallel, and tripled for three rubber bands in parallel.

Model tests were ultimately conducted independently with one, two, and three rubber bands at each corner of the wooden test frame in order to produce three unique values of the system stiffness and in order to produce various values of natural period. For the final mooring system, tests were then conducted with four rubber bands (one at each corner), eight rubber bands (two at each corner), and twelve rubber bands (three at each corner). These rubber bands were all installed with a small initial tension. For these configurations, the total system stiffness was then four, eight, or twelve times the basic stiffness of single rubber band. These values are summarized in Table 2.

Table 2. Stiffness of the Mooring System used in Model Tests

Number of Rubber Bands in Spread Mooring	System Stiffness, K (lbs/ft)
Four in system (one each corner)	2.08
Eight in system (two each corner)	4.16
Twelve in system (three each corner)	6.24

One Rubber Band

K=0.52 lb/ft
for displacements less
than hull width

Two Rubber Bands

K=0.52 lb/ft
per rubber band
for displacements less
than hull width

Three Rubber Bands

K=0.52 lb/ft
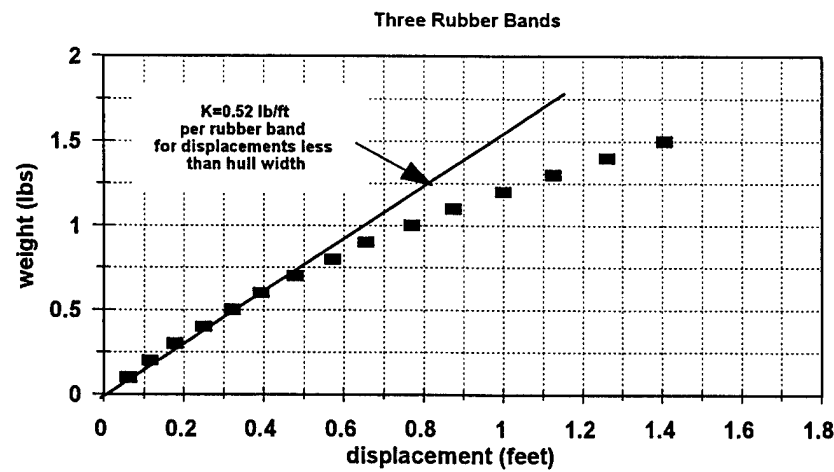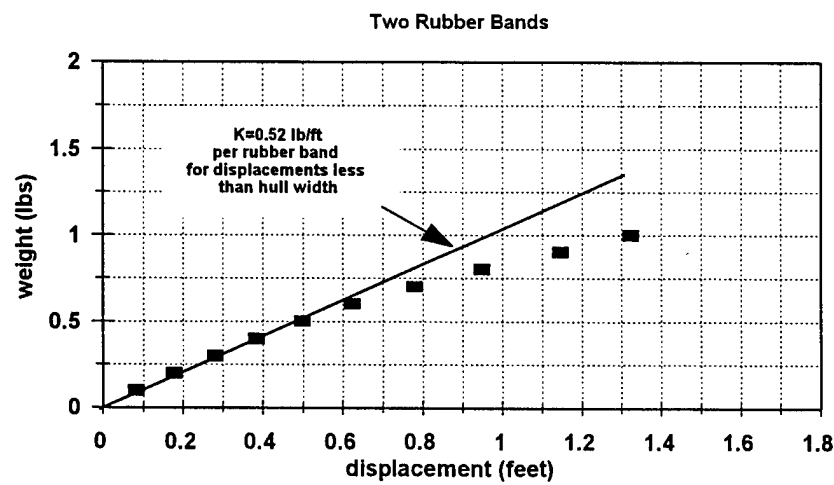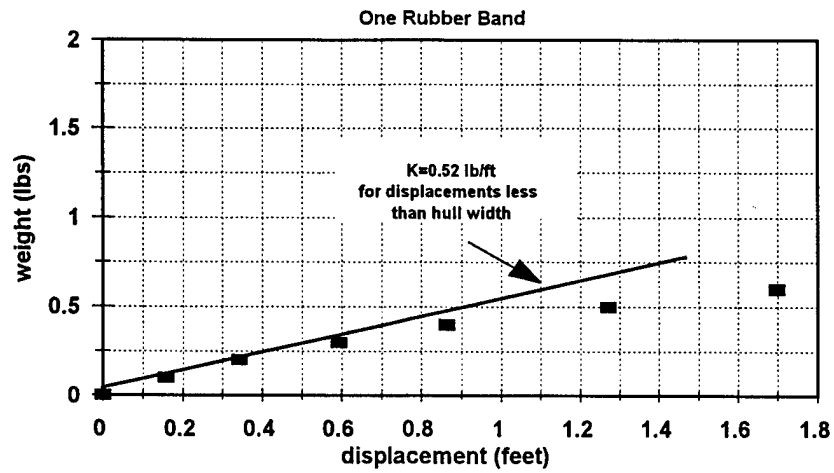per rubber band
for displacements less
than hull width

Figure 2. Determination of stiffness of one, two, and three rubber bands

8

As a check on the system stiffness, additional tests were conducted to document the in-place stiffness of the mooring system in the Stability Tank. One ship was connected to the side walls of the stability tank with one rubber band attached at each of the four corners of the wooden test frame (a total of four bands). Using a hand-held force gage, the model was then displaced, three, six, nine, and twelve inches, and the force required to produce these displacements was recorded. This test was then repeated for two and three rubber bands per attachment (a total of eight and twelve bands). Using the simple equation for a static force balance, $F = K y$, the measured force and displacement were used to calculate the in-place system stiffness. The results of these tests are shown in Figure 3 in which the system stiffness is plotted versus the total number of rubber bands in the system. As may be seen, the experimental values from these simple tests agree quite well with the expected values based on the stiffness of 0.52 lbs/ft per rubber bands as determined from the previous tests.
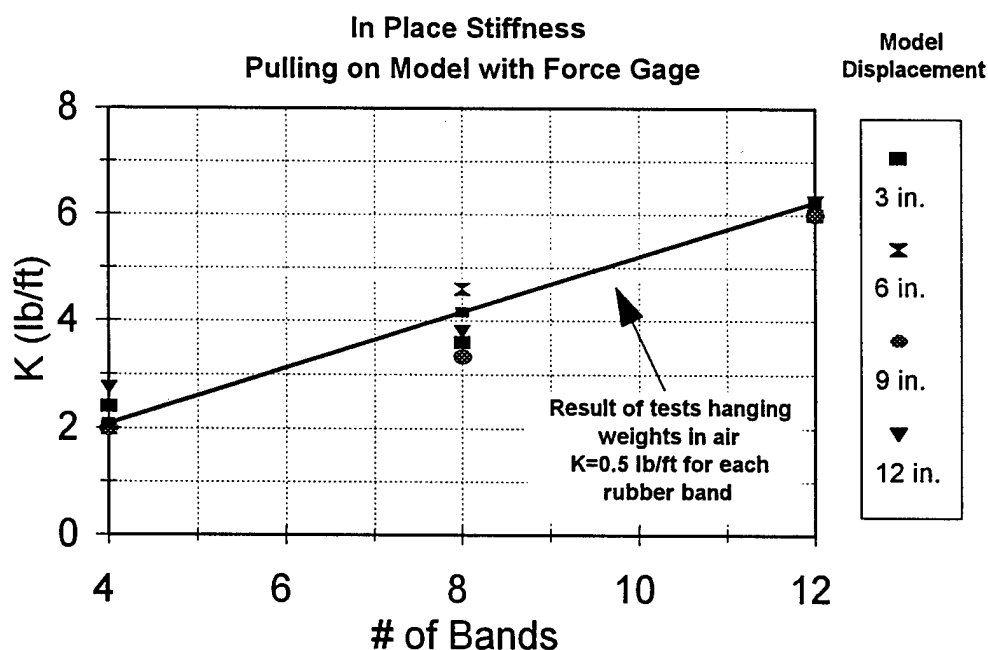

Figure 3. Tests on in-place stiffness using hand-held force gage

Description of Experiments

The experiments were conducted with a test matrix that included 60 tests with systematic changes in three variables: the number of ships moored together, the stiffness of the mooring system, and the water depth. The test conditions, as well as a summary of results for added mass and damping characteristics, as summarized in Table 3.

As noted, tests were conducted with a single ship and with nests of two, three, four, and five ships. These variations produced strong changes in the total mass, the total added mass, and the total damping forces in of the system. As was also noted, tests were conducted with three values of the system stiffness of 2.08, 4.16, and 6.24 lbs/ft. These variations produced a wide range of natural periods near the desired period of 13 seconds. As shown in Table 3, the achieved natural periods ranged from about 6 to 22 seconds with an average of 12.6 seconds.

The third variable, water depth, was varied to produce four values of the draft-to-depth ratio (T/d) of 0.1, 0.5, 0.7, and 0.95. With the four inch draft of the models, the initial depth used in the test was 40.0 inches, which produced $T/d = 0.10$. For this condition, the water depth did not have strong effect on either added mass or damping, and these tests may be considered representative of the limiting deep water condition of $T/d=0$. Other tests were conducted with shallow water depths of 8.0 inches ($T/d=0.5$), 5.7 inches ($T/d=0.7$), and 4.2 inches ($T/d=0.95$). The last test had only 0.2 inches of clearance between the bottom of the tank and the keels of the models. While the floor of the Stability Tank is concrete, the tank floor is not perfectly level or smooth and it is likely (though not measured) that the tank floor has as much as 0.1 inch of variability in elevation that could affect the true under-keel clearance.

Each experiment was conducted very simply, by giving the group of ships and initial sway displacement of about 6 inches and then by measuring the position of the group as a function of time. Measurements of sway motion were made with a sonic positioning sensor and a sensor target. The sonic gage was fixed in place and was lowered from a steel truss that spanned the top of the tank. The gage was then aimed horizontally at a sheet metal target which was attached to the group of ships.

Sway motions were recorded at a sampling rate of 12.79 Hz for 120 seconds. The data record was started with the models initially at rest. The models were then manually pulled to the initial displacement of about 6 inches, held in place for a few seconds, and then released. The release of the models generally occurred 10 to 20 seconds after the start of data collection and, as a result, dynamic oscillations were recorded for 100 to 110 seconds. Most natural periods were in the range of 10 to 20 seconds so that typically 5 to 10 cycles of sway oscillations were recorded and saved in a computer data file.

Table 3
Test conditions and summary of results

Test	T/d	Number Ships	Mass M (lb-s^2/ft)	Stiffness K (lb/ft)	Natural Period Td (sec)	Added Mass Ma/M	Linear Damping β	Nonlinear Damping C_D
1	0.1	1	1.59	2.08	9.3	1.84	0.09	1.43
2	0.1	3	4.60	2.08	16.1	1.95	0.09	1.25
3	0.1	5	7.73	2.08	20.5	1.83	0.11	1.37
4	0.1	2	3.11	2.08	13.3	1.98	0.08	1.30
5	0.1	4	6.16	2.08	18.2	1.81	0.09	1.09
6	0.5	1	1.59	2.08	9.8	2.15	0.10	2.00
7	0.5	3	4.60	2.08	16.0	1.90	0.10	1.25
8	0.5	5	7.73	2.08	20.8	1.92	0.11	1.25
9	0.5	2	3.11	2.08	13.2	1.93	0.09	1.41
10	0.5	4	6.16	2.08	19.0	1.91	0.10	1.41
11	0.7	1	1.59	2.08	10.8	2.80	0.12	2.50
12	0.7	3	4.60	2.08	16.9	2.21	0.13	1.67
13	0.7	5	7.73	2.08	22.0	2.24	0.14	1.50
14	0.7	2	3.11	2.08	14.1	2.33	0.11	1.87
15	0.7	4	6.16	2.08	19.2	2.10	0.13	1.72
16	0.95	1	1.59	2.08	11.3	3.17	0.14	5.00
17	0.95	3	4.60	2.08	20.8	3.80	0.18	4.79
18	0.95	5	7.73	2.08	23.9	2.76	0.19	3.50
19	0.95	2	3.11	2.08	14.6	2.55	0.13	4.68
20	0.95	4	6.16	2.08	22.7	3.27	0.18	4.50
21	0.1	1	1.59	4.16	6.8	2.05	0.07	1.00
22	0.1	3	4.60	4.16	11.1	1.80	0.08	1.04
23	0.1	5	7.73	4.16	14.1	1.69	0.09	1.00
24	0.1	2	3.11	4.16	9.2	1.85	0.07	1.00
25	0.1	4	6.16	4.16	12.8	1.77	0.09	1.09
26	0.5	1	1.59	4.16	7.1	2.32	0.08	1.25
27	0.5	3	4.60	4.16	11.3	1.90	0.10	1.25
28	0.5	5	7.73	4.16	14.7	1.91	0.11	1.12
29	0.5	2	3.11	4.16	8.9	1.67	0.09	1.25
30	0.5	4	6.16	4.16	13.3	1.91	0.10	1.25

Table 3
Continued

Test	T/d	Number Ships	Mass M (lb-s^2/ft)	Stiffness K (lb/ft)	Natural Period Td (sec)	Added Mass Ma/M	Linear Damping β	Nonlinear Damping C_D
31	0.7	1	1.59	4.16	7.6	2.79	0.10	2.50
32	0.7	3	4.60	4.16	12.1	2.33	0.08	1.67
33	0.7	5	7.73	4.16	15.5	2.23	0.12	1.87
34	0.7	2	3.11	4.16	10.1	2.42	0.10	1.87
35	0.7	4	6.16	4.16	13.8	2.21	0.12	2.19
36	0.95	1	1.59	4.16	7.6	2.78	0.11	5.00
37	0.95	3	4.60	4.16	14.7	3.82	0.16	5.00
38	0.95	5	7.73	4.16	16.1	2.46	0.14	4.00
39	0.95	2	3.11	4.16	10.6	2.74	0.13	4.69
40	0.95	4	6.16	4.16	14.6	2.57	0.15	4.22
41	0.1	1	1.59	6.24	5.5	2.00	0.05	1.00
42	0.1	3	4.60	6.24	9.0	1.77	0.07	0.85
43	0.1	5	7.73	6.24	11.2	1.56	0.06	0.75
44	0.1	2	3.11	6.24	7.4	1.77	0.06	1.06
45	0.1	4	6.16	6.24	10.3	1.71	0.08	0.86
46	0.5	1	1.59	6.24	5.8	2.33	0.07	1.25
47	0.5	3	4.60	6.24	9.4	2.02	0.07	1.20
48	0.5	5	7.73	6.24	11.9	1.88	0.08	1.12
49	0.5	2	3.11	6.24	7.7	2.00	0.07	1.12
50	0.5	4	6.16	6.24	10.7	1.96	0.07	1.25
51	0.7	1	1.59	6.24	6.1	2.68	0.09	2.50
52	0.7	3	4.60	6.24	10.1	2.48	0.09	2.20
53	0.7	5	7.73	6.24	12.6	2.20	0.12	2.25
54	0.7	2	3.11	6.24	8.3	2.48	0.09	2.19
55	0.7	4	6.16	6.24	11.3	2.23	0.12	2.34
56	0.95	1	1.59	6.24	6.0	2.58	0.12	5.00
57	0.95	3	4.60	6.24	11.9	3.66	0.20	5.21
58	0.95	5	7.73	6.24	14.1	2.97	0.16	5.00
59	0.95	2	3.11	6.24	8.5	2.59	0.15	5.31
60	0.95	4	6.16	6.24	13.3	3.41	0.17	5.47

Data Analysis Procedure

A sample plot of the sway displacement data is shown in Figure 4 to illustrate the data analysis procedure. The analysis first involved a direct determination of the natural period of the damped oscillations and then involved a subsequent analysis of the damping and added mass. In the first phase, the natural period of motions was determined just after each data run. The computer-based data collection system used in the Hydromechanics Laboratory permits cross-hairs to be easily positioned at the maxima of each dynamic oscillation and for the time of occurrence of each maxima to be displayed. These times (denoted t_1, t_2, etc in Figure 4) were displayed and recorded for the first 5 to 10 oscillations of each test. These were then used to determine the damped natural period, T_d, and the natural frequency, $\omega_d = 2\pi/T_d$. These values are listed in Table 3.

Following this determination of the natural period (frequency), the data were analyzed to determine the linear damping ratio, β, and the dimensionless added mass, M_a/M. This was accomplished using a spreadsheet in which a graph of the measured data was displayed with a graph of the exponential (linear) damping function, $Y_o \exp(-\zeta t)$, superimposed. The initial offset Y_o was known and the value of ζ was then adjusted by trial and error until the exponential function appeared to provide an optimal fit of the upper and lower bounds of the dynamic oscillations. Once ζ was known, the values of ω_n and β were determined from equation (3) and (4). Finally, the added mass coefficient, M_a/M, was determined from equation (7) based on the known system stiffness K and the known total mass of the ships in the group M.
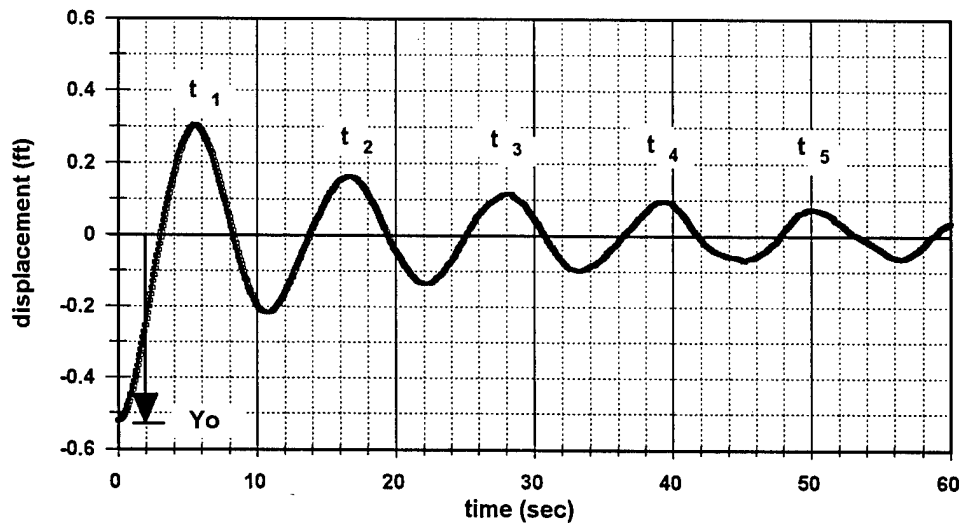

Figure 4. Illustration of damped oscillation

13

The values of β and M_a/M for each test are listed in Table 3. It is noted that the values of β correspond to the linear damping ratio of the entire group of ships. The dimensionless added mass is determined as the added mass of the group of ships relative to the total mass of the group. It may also be interpreted as the average value of M_a/M for any ship in the group. It may be seen from Table3 that the ratio of M_a/M for sway motions was generally found to vary from a low of 1.55 to a high of 3.95, with larger values associated with the largest value of T/d tested.

It is noted that the added mass is formally dependent on the damping ratio of the system, β. In general, however, there is little real dependence of M_a/M on β because the system is found to be very lightly damped. The damping ratio β may be interpreted as the ratio of the actual damping in the system to the critical damping of the system. Values of β range from 0.06 to 0.20 and, for such lightly damped systems, there is no practical dependence of M_a/M on β. In addition, there is no significant difference between the damped and undamped natural frequencies given in equation (3), as the quantity $(1-\beta^2)^{1/2}$ is essentially equal to unity.

As noted previously, the linear (exponential) damping function did not always fit the measured dynamic motions very well. Figure 5 gives an example of a test in which the exponential model is clearly not a good physical representation of the actual decay of the motions. Frequently, the actual amplitudes of the motions would decay very quickly in the first few oscillations and would then decay much more slowly in subsequent oscillations. As a result, an exponential function fitted to match the decay of the first few oscillations would decay completely indicate no motions later in time when the data suggested a finite motion with very slow decay.

In order to provide a better description of the damped motions, the nonlinear quadratic damping model in equation (8) was adopted and values of the quadratic drag coefficient, C_D, were determined. This involved numerically solving equation (8) in finite difference form, starting from initial conditions of the known initial sway displacement, $y = Y_o$, and an initial sway velocity, $\dot{y} = 0$. The numerical solution required input of the system stiffness, K, and the total system mass plus added mass $M + M_a$. In the finite difference solution, the nonlinear damping coefficient of the system, B_{NL}, was then adjusted by trial and error to obtain what visually appeared to be the best fit of the dynamic motions. Figure 6 shows an example of the goodness-of-fit that could be achieved from the finite difference solution of the nonlinear equation of motion.

Once the value of B_{NL} was determined, corresponding values of the average drag coefficient for each ship in the group, C_D, were then computed from equation (9). It is emphasized that these values are reported as the **average value per ship** for a group of ships. Values of C_D are also listed in Table 3 for each test. In general, values of C_D are found to vary between about 0.75 and 5.31, with the largest values associated with the largest value of T/d tested.
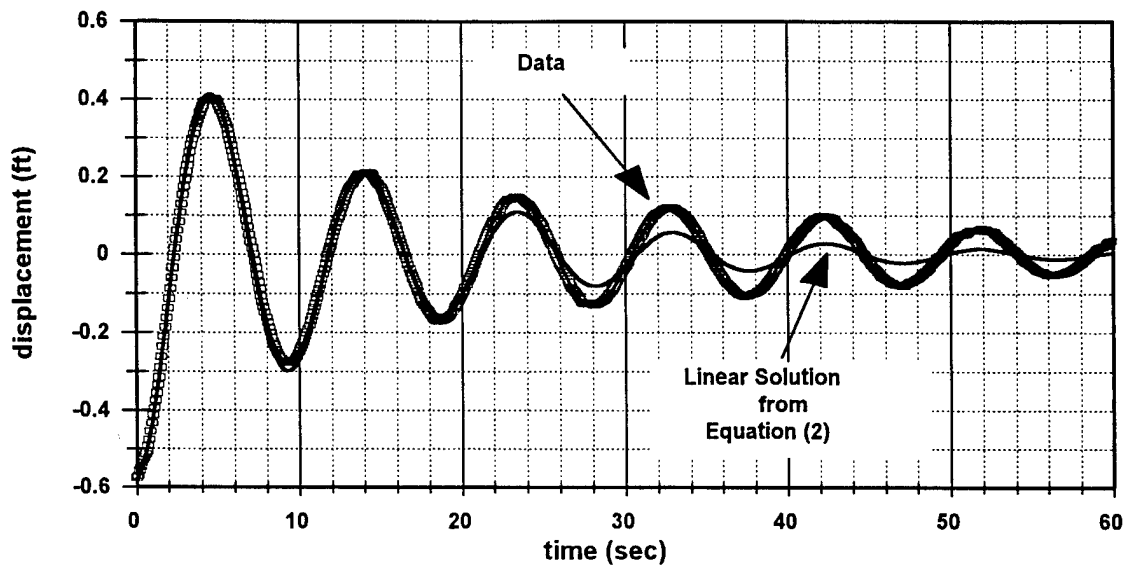
14

Figure 5. Example of simulation using linear equation of motion
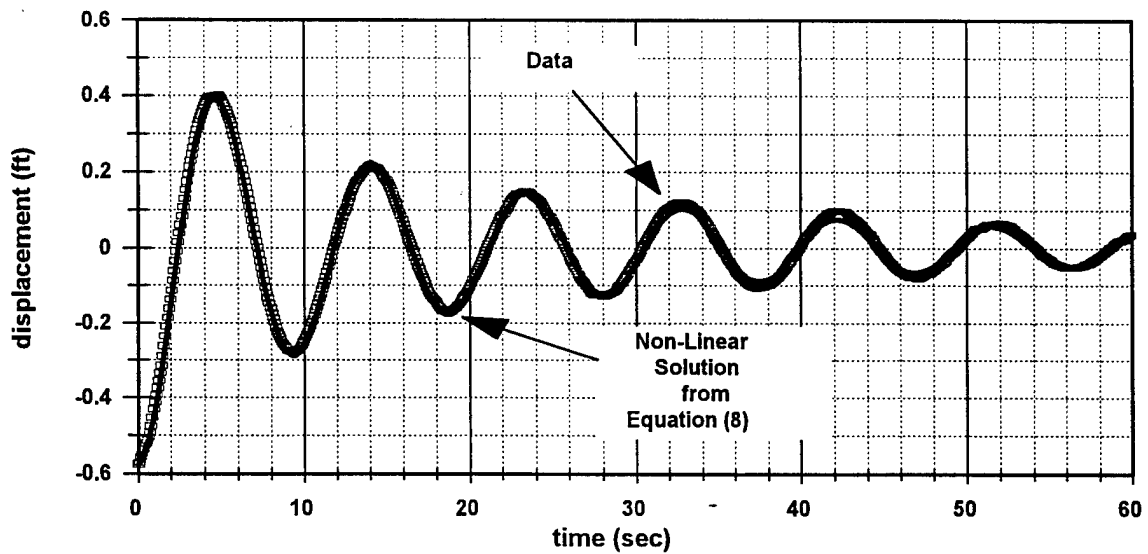with linear (exponential) damping

Figure 6. Example of simulation using non-linear equation of motion
with quadratic damping

15

Analysis of Results

Added Mass

Graphical results for the ratio of M_a/M are shown in Figures 7a and 7b. Analysis of added mass coefficients showed no identifiable dependence of added mass on the stiffness of the system, K. As a result, the results for the three values of stiffness are averaged to produce summary graphs showing the notable dependence of added mass on either: (1) the number of ships in the group or (2) on the draft-to-depth ratio. Additional detail on the behavior of M_a/M with variations in the stiffness are presented in Appendix B.

Added Mass as a Function of Number of Ships

Figure 7a suggests that M_a/M is only weakly dependent on the number of ships in the group and is more strongly dependent on the draft-to-depth ratio, as the variation from curve to curve (different values of T/d) exceeds the variation along any one curve (with number of ships). Along any one curve, the following trend is clearly evident: M_a/M decreases as the number of ships increases. For the deep water case, $M_a/M = 2$ for a single ship and then decreases to 1.65 per ship for the nest of 5 ships. Similar trends are found for T/d values of 0.5 and 0.7, with clear trends toward decreasing M_a/M for increasing numbers of ships in the group. Once again, it is emphasized that results are presented in dimensionless (normalized) form. If the actual mass and added mass were separately considered, then both M and M_a would increase considerably as the number of ships increases.

The trend for T/d=0.95 is more difficult to discern, due to the large scatter in the experimental values of added mass. These test data were by far the most difficult to analyze. For this extreme shallow water condition, it was visually evident that the dynamic motions were not smoothly damped sinusoidal motions at a single frequency. Often, the models were observed to be oscillating in coupled sway-yaw motions so that the resulting time series showed a combination of sway natural frequencies and yaw natural frequencies. In addition, energy transfers occurred between the modes in which sway motions would decay quickly while yaw motions would increase, and then, later in time, the yaw motions would decay quickly and sway motions would increase again. These coupled sway-yaw motions in shallow water were also showed visible vortex formation at bow and stern. Because of these characteristics, it was very difficult to precisely determine the sway natural period and the damping rate. The result is significant uncertainty and scatter in the experimental values as, for example, the added mass was noticeably higher for three ships than for either two or four ships.

AVERAGED OVER ALL K VALUES

Top chart axes: Ma/M (y-axis, 0 to 4) vs # of ships (x-axis, 1 to 5)

Legend: T/d=0.1, T/d=0.5, T/d=0.7, T/d=0.95

Bottom chart axes: Ma / M (y-axis, 0 to 4) vs Draft / Depth (x-axis, 0 to 1)

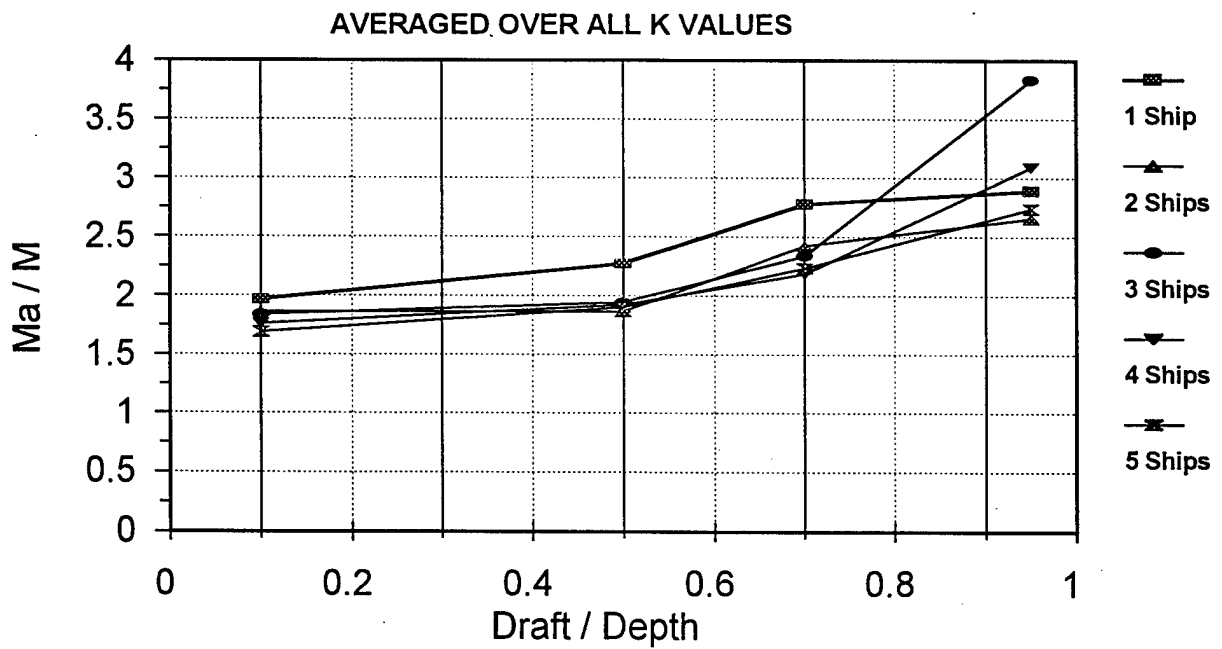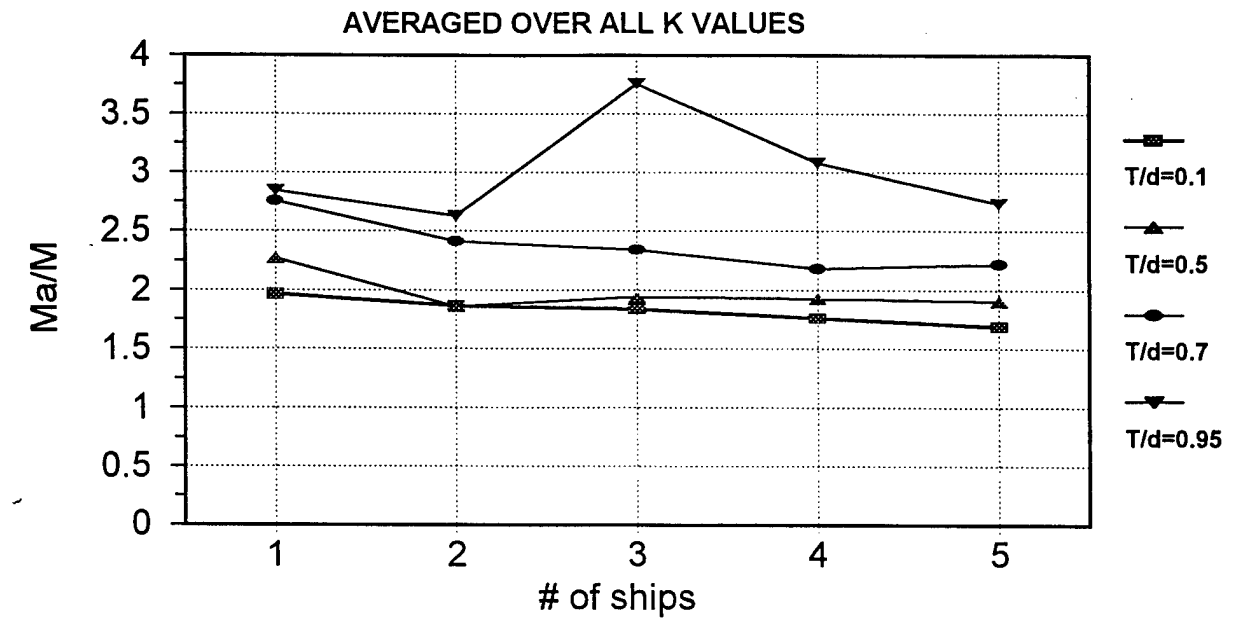Legend: 1 Ship, 2 Ships, 3 Ships, 4 Ships, 5 Ships

Figure 7a (top) and 7b (bottom) showing results for added mass

The downward trend in M_a/M with increased numbers of ships in the group may be explained in simplified physical terms by the sheltering provided by multiple ships. If the added mass physically represents a mass of water surrounding a ship which is accelerated by the moving ship, then the addition of a second ship alongside the first ship acts to effectively trap a finite mass of water between the ships. Because of the "overlap" of added mass between the ships, the total added mass of the two nested ships is smaller than that which would be obtained if the ships had a wider separation distance. As a result, while the addition of a second identical ship would double the total ship mass in the system, it does not double the added mass.

Added Mass as a Function of T/d

Figure 7b shows M_a/M (averaged over the three stiffness values) plotted as a function of T/d with five curves corresponding to the number of ships in the mooring group. In this format, it is clear that there is a strong increase in added mass as T/d increases, while there is a small decrease in added mass as the number of ships increases.

For one ship, M_a/M equals about 2 for the case with the largest water depth and then increases to more than 2.8 for the case of $T/d = 0.95$. Similar strong trends are observed for any number of ships: as the draft-to-depth ratio approaches unity, the added mass can increase by 50% to nearly 100% from the value found in the deep water tests. The values of M_a/M added mass obtained for one ship are generally higher than those obtained for any other number of ships in a group. Results for 2 or more ships in a group are then consistent with each other with M_a/M equal to about 1.8 for the largest water depth and then increasing to 2.0 and 2.3 for T/d of 0.5 and 0.7 respectively. Data scatter then makes simple conclusions difficult for $T/d = 0.95$.

Added Mass - Conclusions

1. As the number of ships in a group of moored ships increases, the added mass-to- mass ratio decreases slightly.

2. As the depth of water decreases and approaches a draft-to-depth ratio of unity, the added mass-to-mass ratio approximately doubles from that found in deep water.

3. The added mass-to-mass ratio is not frequency dependent for the range of frequencies considered in this study.

18

Linear Damping Analysis

Graphical results for the linear damping ratio, β, are shown in Figures 8a and 8b. The damping ratios shown are again obtained by averaging results over the three values of stiffness, K. Unlike the added mass, β varied somewhat with changes in stiffness, and details of the variation of β with stiffness are shown in Appendix C. As may be seen in those figures, β generally decreased as stiffness increased. Since natural frequency increases with stiffness, it is then found that β also decreased as the natural frequency increased. In order to simplify the graphical presentation of the data, the variation with stiffness is removed by averaging results for the three values of stiffness tested and, Figure 8a and 8b then summarize the remaining dependence of the linear damping ratio on either: (1) the number of ships in the group or (2) on the draft-to-depth ratio.

Linear Damping Ratio as a Function of Number of Ships

Figure 8a suggests that β is only weakly dependent on the number of ships in the group but is strongly dependent on the draft-to-depth ratio. This result is similar to that obtained for the added mass. Unlike the results for added mass, however, it is found that the damping ratio increases as the number of ships increases. For the deep water condition, β increases from about 0.07 for one ship to 0.09 for 5 ships. This trend is also found for other draft-to-depth ratios until, for T/d=0.95, the damping ratio increasing from about 0.12 to more than 0.16 for 1 to 5 ships respectively.

It is noted that even though the dimensionless damping ratio β increases as the number of ships increases, the actual (dimensional) damping rate of the system, $\zeta = \beta \omega_n$, decreases as the number of ships increases. This is shown in Figure 9 as a function of the number of ships in the group. This difference in the way that β and ζ behave is caused by the large change in the natural frequency with an increasing number of ships. By comparing Figure 8a to Figure 9, it is apparent that the decrease in natural frequency associated with adding more ships to the group has a very strong effect on the damping coefficient, leading to a decrease in the quantity $\beta \omega_n$ as the number of ships in the group (and as β) increases.

Linear Damping Ratio as a Function of Draft-to-Depth Ratio

Figure 8b shows that β exhibits a strong increase as the draft-to-depth ratio increases. For any particular number of ships in the group, it is apparent that the damping ratio roughly doubles between the deepest and shallowest depths tested. This strong increase in damping as the underkeel clearance is reduced is similar to the trend observed for added mass.
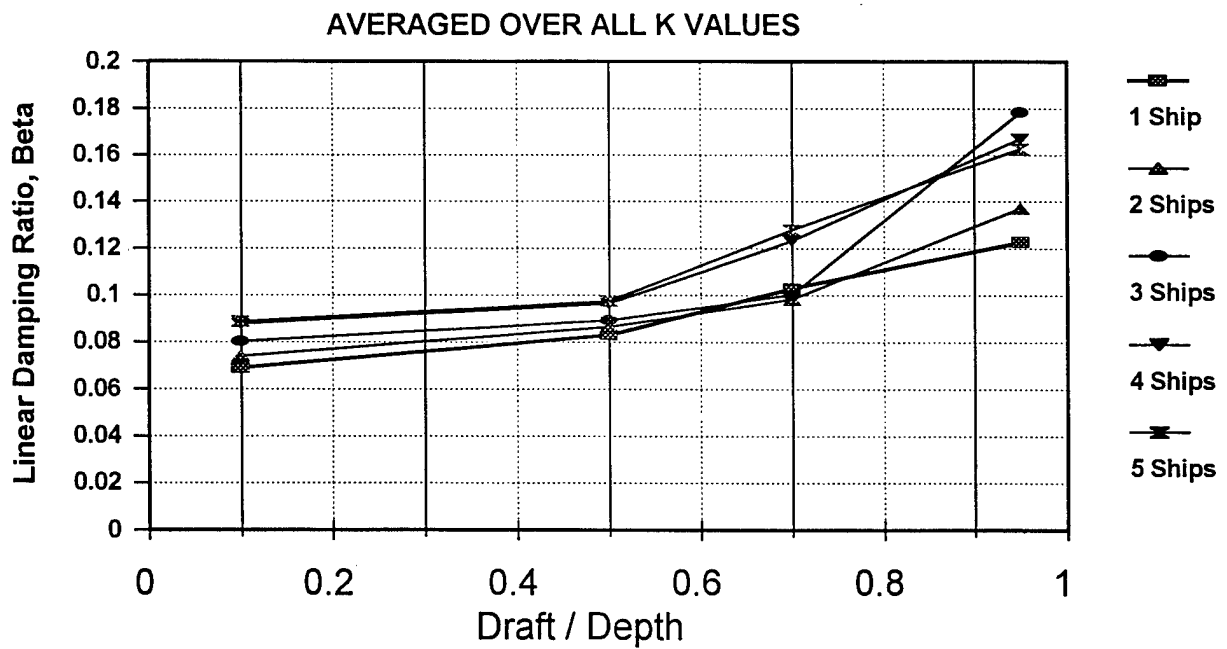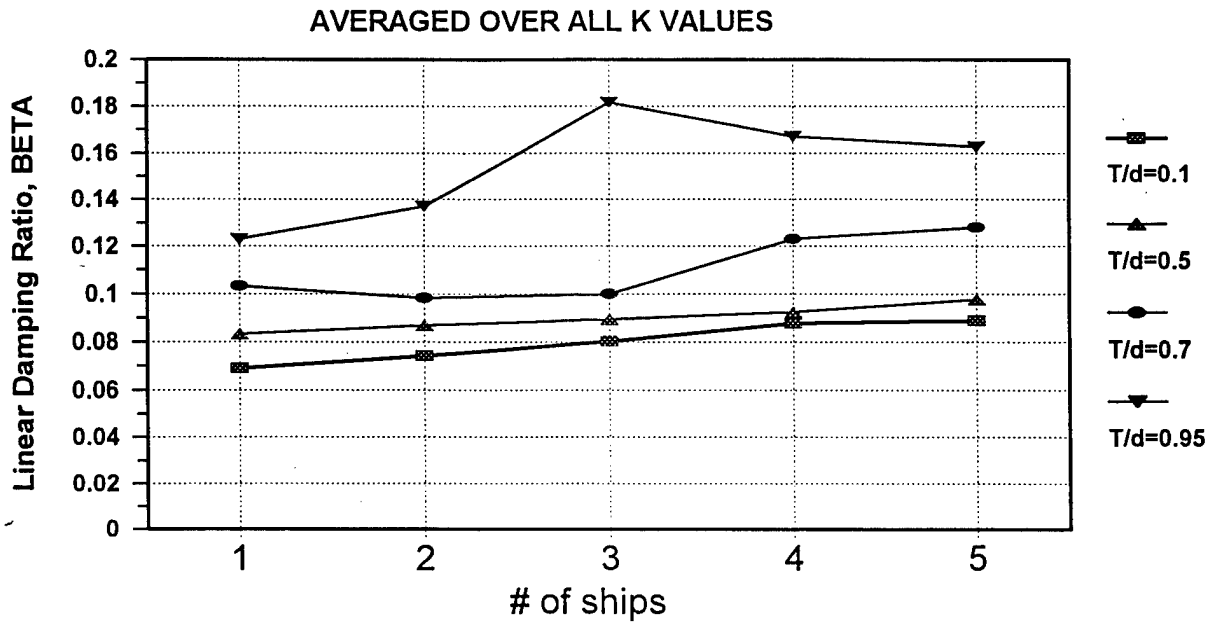
19

AVERAGED OVER ALL K VALUES

AVERAGED OVER ALL K VALUES

Figure 8a (top) and 8b (bottom) showing linear damping ratio, β

20

AVERAGED OVER ALL K VALUES

Legend:
- T/d=0.1
- T/d=0.5
- T/d=0.7
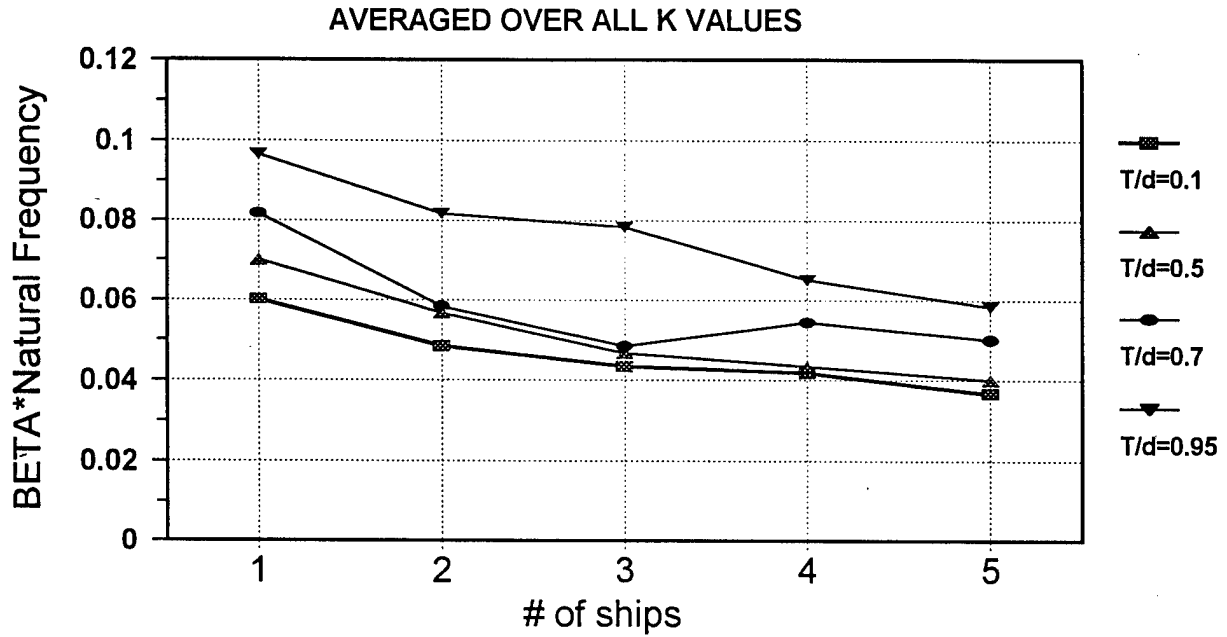- T/d=0.95

Y-axis: BETA*Natural Frequency

X-axis: # of ships

Figure 9 Linear damping rate, $\zeta = \beta \, \omega_n$

Linear Damping Ratio - Conclusions

1. As the number of ships in a group of moored ships increases, the dimensionless linear damping ratio, β, increases slightly while the dimensional damping rate, $\beta\omega_n$, decreases. The difference between these two results reflects the strong decrease in natural frequency that occurs by adding new ships to the group.

2. As the depth of water decreases and approaches a draft-to-depth ratio of unity, the linear damping ratio, β, approximately doubles from that found in deep water. This is the same trend found for added mass.

3. The linear damping ratio, β, is weakly frequency dependent for the range of frequencies considered in this study. Data scatter makes definitive conclusions about the variation with frequency difficult to discern but generally β decreases as stiffness (natural frequency) increases.

21

Non-Linear Damping Analysis

Graphical results for the nonlinear quadratic damping used in equation (8), expressed in terms of the cross-flow drag coefficient, C_D, are shown in Figures 10a and 10b. These drag coefficients are obtained from equation (9) as

$$C_D = \frac{B_{NL}}{N \frac{1}{2} \rho L T}$$

(9)

where B_{NL} is the dimensional damping coefficient obtained for the entire group of ships and where C_D is then defined as the average drag coefficient per ship in the group of moored ships. These drag coefficients are obtained by averaging results over the three values of stiffness, K. Details of the variation of C_D with changes in stiffness are given in Appendix D. In general, C_D is not strongly dependent on the stiffness (natural period) of the system and no systematic variation of C_D on K may be found. As a result, the variation with stiffness is removed by averaging results for the three values of stiffness tested and, Figures 10a and 10b then summarize the remaining dependence of the linear damping ratio on either: (1) the number of ships in the group or (2) on the draft-to-depth ratio.

Quadratic Drag Coefficient as a Function of Number of Ships

Figure 10a shows that C_D is only weakly dependent on the number of ships in the group and is more strongly dependent on the draft-to-depth ratio. Like the results for added mass, the drag coefficient decreases slightly as the number of ships increases. For the deep water condition, C_D decreases from about 1.2 to 1.05 as the number of ships in the group is varied from one to five. This trend is also found for other draft-to-depth ratios until, for T/d = 0.95, C_D decreases from 5.0 to 4.2 for one to five respectively.

Quadratic Drag Coefficient as a Function of Draft-to-Depth Ratio

Figure 10b shows the strong increase in C_D as the draft-to-depth ratio increases. For any particular number of ships in the group, it is apparent that the drag coefficient can increase by a factor of four to five between the deepest and shallowest depths tested. This relative increase in the drag coefficient as the underkeel clearance is reduced is even stronger than the trend observed for added mass.
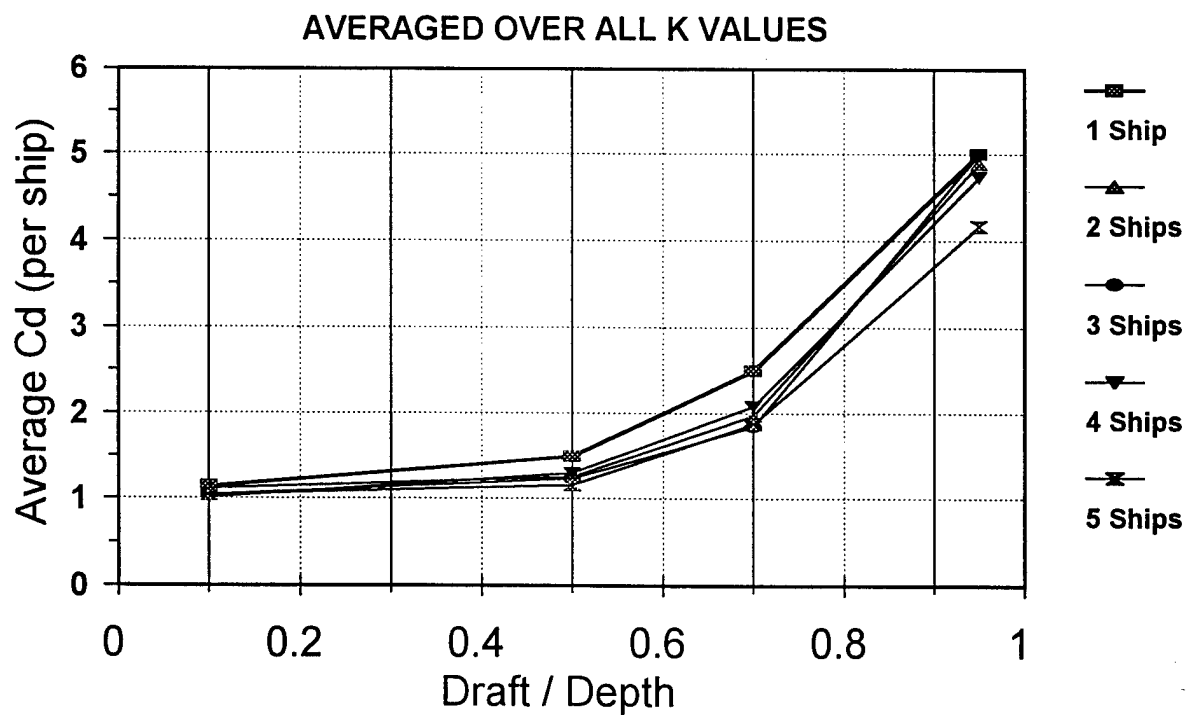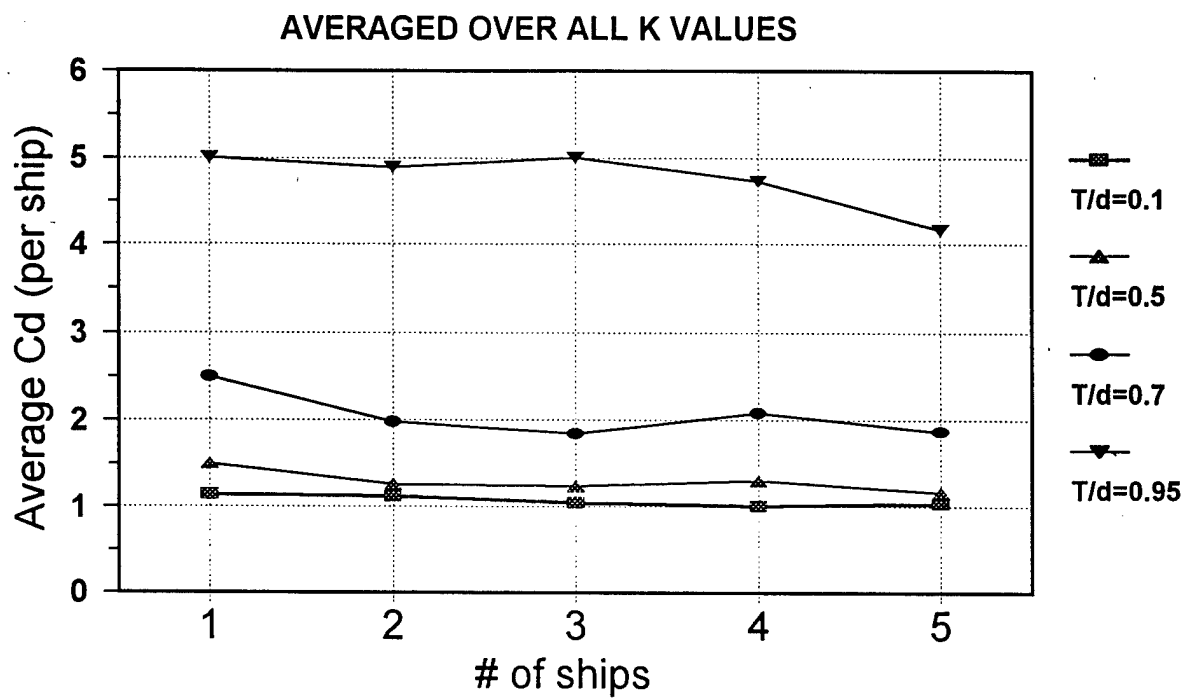
Figure 10a (top) and 10b (bottom) showing cross-flow drag coefficient C_D

1. As the number of ships in a group increases, the dimensionless drag coefficient C_D decreases by a few percent. Application of the drag coefficient for one ship to each ship in a group will therefore result in an over-estimate of damping for the system.

2. As the depth of water decreases and approaches a draft-to-depth ratio of unity, the drag coefficient C_D increases by a factor of more than four from that found in deep water. This is a stronger variation than was found for added mass or for the linear damping ratio.

3. The drag coefficient may be weakly dependent on the natural frequency (stiffness) of the system, but no obvious trend was evident.

Summary

Results of this study provide some guidance on the added mass and damping characteristics for a "nest" of multiple moored ships in shallow water. Results generally suggest that, for a nest of ships, the added mass and damping do not increase directly in proportion to the number of ships in the group. Some "sheltering" occurs such that the added mass and damping of the entire group of N is somewhat less than N times the added mass or damping of a single ship. This sheltering effect is not too pronounced, however, and leads to roughly a 10 percent decrease in total added mass as the number of ships increases from one to five. Much stronger effects are found in shallow water as the water depth decreases. In this cases, the added mass can nearly double from deep water to a draft-to-depth ratio of 0.95; the quadratic damping coefficient can increase nearly four fold from deep water to the shallowest depth tested to a draft-to-depth ratio of 0.95.

Recommendations for further experimental work could included several parametric studies to better define the effects of multiple ships or of shallow water. First, the present study considered only the sway motions; additional work could consider surge motions or yaw motions. As noted in this report, the sway and yaw motions became strongly coupled in shallow water. Second, the effects of shallow water could also be investigated in greater detail. This study considered three shallow water conditions, but there was significant data scatter at the shallowest condition at a draft-to-depth ratio of 0.95. As a result, additional investigation may be warranted into the behavior at draft-to-depth ratios of 0.8 to 0.95. Third, additional investigations into the response of different ship hull forms could be of interest. This study considered a naval training ship and additional investigations into naval combatants would be of interest.
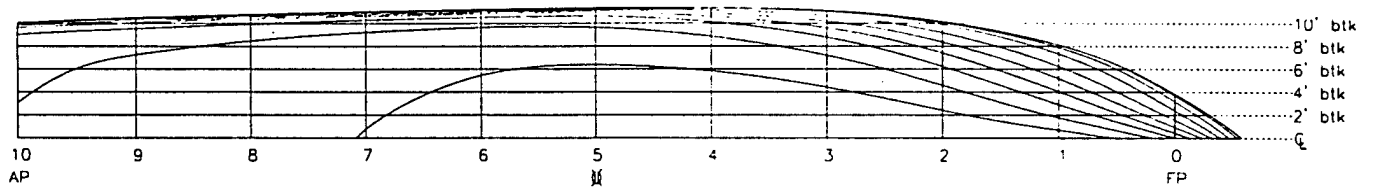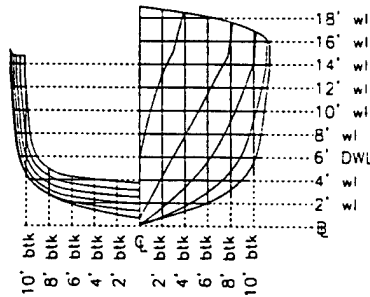
Acknowledgements
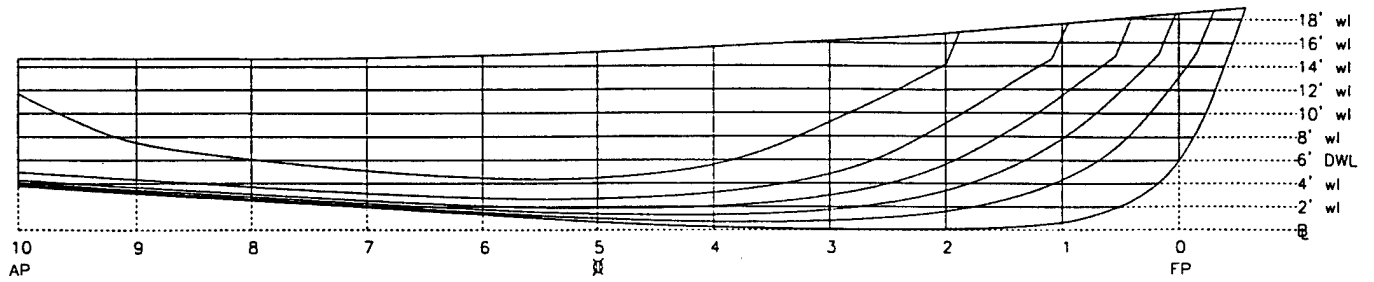
Appendix A

Sheer Plan

Half Breadth Plan

Body Plan

Principal Dimensions	
LOA	107' 4"
LPP	101' 8"
Beam Max	22' 9"
Station Spacing	10' 2"
Draft	6' 0"

26

Draft / Depth = 0.7

K=2.08 lb/ft

K=4.16 lb/ft

K=6.24 lb/ft

AVERAGE

Draft / Depth = 0.95

K=2.08 lb/ft

K=4.16 lb/ft

K=6.24 lb/ft

AVERAGE

Appendix B

Draft / Depth = 0.1

Draft / Depth = 0.5

27

Appendix C

Draft / Depth = 0.1

Linear Damping Ratio, BETA vs. # of ships

- K=2.08 lb/ft
- K=4.16 lb/ft
- K=6.24 lb/ft
- AVERAGE

Draft / Depth = 0.5

Linear Damping Ratio, BETA vs. # of ships

- K=2.08 lb/ft
- K=4.16 lb/ft
- K=6.24 lb/ft
- AVERAGE

29

Draft / Depth = 0.7

Draft / Depth = 0.95

Appendix D

Draft / Depth = 0.1

Draft / Depth = 0.5

31

Draft / Depth = 0.7

Draft / Depth = 0.95